Journal homepage: http://www.journalijar.com

RESEARCH ARTICLE

Oxidative Chemical Polymerization of Ortho-Tolidine in Acid Medium Using $K_2Cr_2O_7$ as Oxidizing Agent and Characterization of the Obtained Polymer

Said. M. Sayyah[1*], Ahmed A. Aboud[2], Amgad. B. Khaliel[1] and Salama. M. Mohamed[1].

1. Polymer Research Laboratory, Chemistry Department, Faculty of Science, BeniSuef University 62514 Beni-Suef, Egypt.
2. Physics Department, Faculty of Science, Beni Suef University 62514 Beni-Suef, Egypt

Manuscript Info	*Abstract*
	Potassium dichromate initiated polymerization of o-tolidine in acidified aqueous medium was carried out. The effects of potassium dichromate, hydrochloric acid and monomer concentrations on the polymerization reaction were investigated. The order of reaction with respect to potassium dichromate, hydrochloric acid and monomer concentration was found to be 0.927, 0.984 and 1.086 respectively. Also, the effect of temperature on the polymerization rate was studied and the apparent activation energy of the polymerization reaction was found to be 59.26 kJ/mol. A molecular mechanism for the oxidation of o-tolidine using potassium dichromate is proposed. This mechanism explains the specific features of o-tolidine oligomerization and polymerization. The obtained polymer was characterized using XPS, IR, UV-visible and elemental analysis. The surface morphology of the obtained polymers was characterized by X-ray diffraction and transmission electron microscopy (TEM). The TGA analysis was used to confirm the proposed structure and number of water molecules in each polymeric chain unit. The ac conductivity (σac) of (POTO) was investigated as a function of frequency and temperature. The microscopic conduction mechanism of charge carries over the potential barrier in polymer backbone is classical hopping model.

INTRODUCTION

Intrinsically conductive polymers (ICPs) have become an efficient alternative to inorganic conductors in many practical applications in the recent decade (E. Hrehorova, (2007)). Polyaniline has been an important member in the ICP family, owing to its ease of preparation, excellent environmental stability, various forms, interchangeable oxidation states, electrical, optical properties and economic cost (P. Wang., (2013)), (Jaymand., (2013)) and (X. Guo., (2013)). It has various potential applications; in many high performance devices such as rechargeable batteries (Y. Zhao., (2013)), chemical sensors (C. Steffens., (2014)), (L. Wang ., (2014))electromagnetic shielding (Yo. Moon., (2013)), electrochemical and corrosion devices (G. Gupta ., (2013)), (A. R. Elkais ., (2013)). A common feature of conducting polymer is conjugation of π-electrons extending over the length of the polymer backbone (K.Müllen., (2013)). The common synthesizing method of conducting polymers, namely: chemical oxidative (N. Gospodinova, (1998)) or electrochemical (K. Gurunathan, (1999)) polymerization. Various chemical oxidizing agents, such as potassium dichromate (P.Chowdhury, (2005)) potassium iodate (R.Hirase., (2004)) hydrogen peroxide (K. Gopalakrishnan., (2012)) ferric chloride or ammonium persulphate was used (K.Molapo., (2012)). The applications of polyaniline are limited due to its poor processability (Y.Cao., (1992)), which is true for most conducting polymers. Several studies have been done in order to improve the solubility of polyaniline, among them, using functionalized protonic acids as dopant, like p-toluene-sulphonic acid, octyl-benzene-sulphonic acid, dodecyl benzene-sulphonic acid (A.Heeger, (1993)), poly(styrene) sulphonic acid (Y.Kang., (1992))and phosphoric

acid esters (A.Pron., (1998)). An alternative method to obtain soluble conductive polymers is the polymerization of aniline derivatives. The investigated aniline derivatives are alkyloxy, hydroxy, chloroaniline and substitution at the nitrogen atom was reported by (S.M.Sayyah. H. A.-E., (2005)) (Sayyah, Bahgat, & Abd El Salam, (2002)) (S.M.Sayyah, (2001)) (S.M.Sayyah. H. A., (2003)) to improve the solubility of polyaniline. The substituted group of aniline affects not only the polymerization reaction but also the properties of the polymer obtained. The kinetics of chemical polymerization of 3-methylaniline, 3-chloroaniline, 3-hydroxyaniline , 3-methoxyaniline and N-methyl aniline in hydrochloric acid solution using sodium dichromate as oxidant and characterization of the polymer obtained by IR, UV-visible and elemental analysis, X-ray diffraction , scanning electron microscopy, TGA-DTA analysis and ac conductivity have been reported by (S.M.Sayyah. A. A., (2001)) (S.M. Sayyah. H. A., (2002)) (S.M.Sayyah. A. B., (2002)) (S.M. Sayyah. A. A., (2001)). Carbon nanotubes have been recognized as one of the most versatile materials of the new century. This class of material has generated intense interest in the scientific community for a host of applications, ranging from large scale to nano-scale structures (P.Bandaru., (2007)). Carbon nanotubes are a popular adsorbent for removing of broad range organic and inorganic contaminants from air, soil and liquids. Its high sorption capacity is due to its abundant pores and large internal surface area. CNTs exhibit many superior properties that are promising for several applications and the introduction of CNTs in polymer matrices represents a new direction for the development of composite materials in a wide of applications. This is due to the combined exceptional properties exhibited by the composites cannot be found in the individual constituent materials (P.S. Goh ., (2014)).

The present work intends to study the solubility and kinetics of the oxidative chemical polymerization of o-tolidine in aqueous HCl medium and potassium dichromate as oxidant. The obtained polymer is characterized by XPS, IR, UV-visible, TGA, elemental analysis, X-ray, transmission electron microscopy (TEM) and ac conductivity measurements. Also composite of multi-walled carbon nano-tubes (MWCNTs)/(POTO) was prepared by drop wise chemical polymerization method with HCl as the dopant and $K_2Cr_2O_7$ as the oxidant.

Experimental

2.1- Materials:

O-tolidine provided by Honeywell Chemical Co., (Germany). Concentrated hydrochloric acid, pure grade product, provided by El-Nasr pharmaceutical chemical Co., Egypt. Potassium dichromate provided by Sigma-Aldrich chemical Co., (Germany). Doubly distilled water was used to prepare all the solutions needed in the kinetic studies.

2. 2- Oxidative Aqueous Polymerization of O-tolidine Monomer:

The polymerization reaction was carried out in a well-stopped conical flask of 250 ml capacity; addition of OTO amount in 25 ml HCl of known molarity followed by the addition of the required amount of potassium dichromate as oxidant in water (25 ml) to the reaction mixture. The orders of addition of substances were kept constant in all the performed experiments. The stoppered conical flasks were then placed in an automatically controlled thermostat at the required temperature. The flasks were shaken (15 shakings/10 s/15 min) by using an automatic shaker. The flasks were filtrated using a Buchner funnel, and then the obtained polymer was washed with distilled water, and finally dried till constant weight in vacuum oven at 60 $^{\circ}$C.

2.3- Poly- o-Tolidine / Carbon Nano Tube Nanocomposite Preparation:

The multi-walled carbon nano-tubes was prepared as published by (M. Bahgata, 2011).The MWCNTs /(POTO) composite was prepared by drop wise chemical polymerization method with HCl as the dopant and $K_2Cr_2O_7$ as the oxidant. The amount of multi-walled carbon nano-tubes was first mixed with 0.3M $K_2Cr_2O_7$ as oxidant by continuous stirring. The monomer amount of o- tolidine was mixed with 0.2 M HCl solution. The weight ratio of o-tolidine: CNTs was 1:1 .The monomer solution was added drop wise into carbon nano-tubes mixture under ultrasonication and vigorous stirring. The reaction mixture was subsequently kept under stirring for 2 hrs in an ultrasonic water bath. The precipitate was filtered, and washed thoroughly with deionized water. Finally, the precipitate (composite) was dried in vacuum at 60 °C.

2.4- Elemental Analysis, Infrared and Ultraviolet Spectroscopy:

The carbon, hydrogen and nitrogen contents of the prepared polymer were carried out in the micro analytical laboratory at Cairo University by using oxygen flask combustion and a dosimat E415 titirator (Switzerland).

The infrared spectroscopic analysis of the prepared polymer was carried out in the micro analytical laboratory at Cairo University by using a Shimadzu FTIR-430 Jasco spectrophotometer and KBr disc technique.

The ultraviolet-visible absorption spectra of the monomer and the prepared polymer sample were measured using Shimadzu UV spectrophotometer (M 160 PC) at room temperature in the range 200-400 nm using dimethylformamide as a solvent and reference.

2.5 - X-Ray Photoelectron Spectroscopy (XPS).

An XPS spectrum was obtained on XPS-thermo scientific spectrometer, Model: K-ALDH in Central metallurgical research and development institute (CMRDI). Polymer was mounted on a standard sample holder using double-sided adhesive tape. Survey and XPS spectra were obtained with Al Kα monochromatic X-ray with the resolution of 0.7eV.

2.6 -Thermal Gravimetric Analysis (TGA), Transmission Electron Microscopy (TEM) and X-Ray Analysis:

Thermal gravimetric analysis (TGA) of the polymer sample was performed using a SHIMADZU DT-30 thermal analyzer. The weight loss was measured from ambient temperature up to 600 ^{0}C at rate of 20 ^{0}C /min to determine the rate of degradation of the polymer.

X-Ray diffractometer (philip1976.model1390) was used to investigate the phase structure of the polymer powder under the following condition which kept constant during the analysis processes Cu: X-ray tube, scan speed =8/min, current=30mA, voltage =40kv and preset time=10s.

The inner cavity and wall thickness of the prepared polymer was investigated using transmission electron microscopy (TEM) JEOL JEM-1200 EX Π (Japan).

2.7 –Dielectric Measurements:

The dielectric properties of the prepared polymer was estimated based on the dielectric constant (έ) , dielectric loss (ε'') and Ac conductivity σ_{ac} were measured for 0.2cm thick pellet of the prepared powder using Philips RCL bridge (digital and computerized) at a frequency range 12 to 10^5 Hz and over temperature range 30 – 80 ^{0}C using silver as an electrode.

The values of the dielectric constant were determine using standard geometric technique in which the capacitance (C) was assumed to be given by the usual expression for a parallel plate capacitor i.e using formula:

$$\acute{\varepsilon} = \frac{Cd}{\varepsilon_0 A} \tag{1}$$

Where ε_o is the permittivity of vacuum, A is the area of the sample and d is the sample thickness.

The dielectric loss ε'' was calculated from the measurements of the loss factor D and έ using the following relation:

$$\varepsilon'' = D\,\acute{\varepsilon} \tag{2}$$

The ac conductivity was measured using Philips RCL Bridge (digital and computerized) at a frequency range 0.1 – 100 k Hz and at temperature range 30 – 80 ^{0}C. The temperature was controlled by the use of a double wound electric oven.

The ac conductivity σ_{ac} value was calculated using the relation:

$$\sigma_{ac} = \varepsilon''\omega\varepsilon_0 \tag{3}$$

Where $\omega = 2\pi f$ and f is the applied frequency.

2.8 -Calculations:

2.8.1. Determination of Conversion Yield:

The conversion yield of the monomer to the polymer was determined by the weighing of the dry obtained polymer (P) divided by the weight of the monomer (w) and was calculated in the following way:

$$\text{Conversion yield} = \frac{Polymer\ Yield(P)}{Weight\ of\ Momoner\ (w)} \tag{4}$$

2.8.2. Determination of the Polymerization Rate:

The rate of polymerization was determined in the following:

$$\text{Rate}(R_i) = \frac{P}{V \times M.\,wt\,x t}\ (\text{gmol / L.sec}) \tag{5}$$

Where P is the weight of polymer formed at time (t) in seconds, V is the volume of the reaction solution in liters and M.wt is the molecular weight of the monomer.

2.8.3. Calculation of the Apparent Energy of Activation.

The apparent activation energy (E_a) of the aqueous polymerization reaction was calculated using the following Arrhenius equation:

$$\text{Log}(K) = \frac{-Ea}{2.303RT} + C \tag{6}$$

Where K is the rate, R is the universal gas constant, T is the reaction temperature and C is constant.

2.8.4. Determination of Enthalpy (Δ H*) and Entropy (ΔS*):

Enthalpy of activation (ΔH^*) and entropy (ΔS^*) were calculated using transition state theory equations (Eyring equation):

$$K = \frac{RT}{Nh} e^{\Delta S^*/R} . e^{-\Delta H^*/RT} \tag{7}$$

Where K is the rate constant, N is the Avogadro's number, R is the universal gas constant and h is planks constant.

By dividing the above equation by T and taking its natural logarithm we obtain the following equation:

$$\mathrm{Ln}\left(\frac{K}{T}\right) = Ln\frac{R}{Nh} + \frac{(\Delta S^*)}{R} + \frac{(-\Delta H^*)}{RT} \tag{8}$$

A plot of Ln (k/T) against 1/T is linear, with a slope equals to ($-\Delta H^*$/R) and intercept equals to (Ln. k/h + ΔS^*/R). Therefore ΔH^* and ΔS^* can be calculated from the slope and intercept, respectively

3. Result and Discussion:

3.1. Determination of the optimum polymerization conditions:

To optimize the condition for polymerization of o-tolidine, the concentrations of potassium dichromate, hydrochloric acid and monomer were investigated with keeping the total volume of the reaction mixture constant at 50 ml.

3.1.1. Effect of potassium dichromate concentration:

Both of the monomer and HCl concentrations are kept constant at 0.1 M while the oxidant concentrations were varied from 0.1 to 0.5M at 5±0.2°C to investigate the optimum polymerization condition of $K_2Cr_2O_7$. The yield –time curve was represented in figure (1). From which it is clear that, obtained yield increased with the increase of $K_2Cr_2O_7$ reaching maximum value at 0.3M then decreases from 0.3M to 0.5M. This could be due to the fact that, the produced initiator ion radical moieties activate the backbone and simultaneously produced the o-tolidine ion radical, which takes place immediately and therefore, yield increases with the increase of potassium dichromate concentration up to 0.3M. But in the range from 0.3M to 0.5M, the polymer yield decreases up to 0.5M may be due to a high concentration of oxidant promote the formation of low molecular weight oxidation product and also degrade the produced polymer which is easily soluble in water (P.Chowdhury, (2005)), (S. M. Sayyah A. B., (2014))
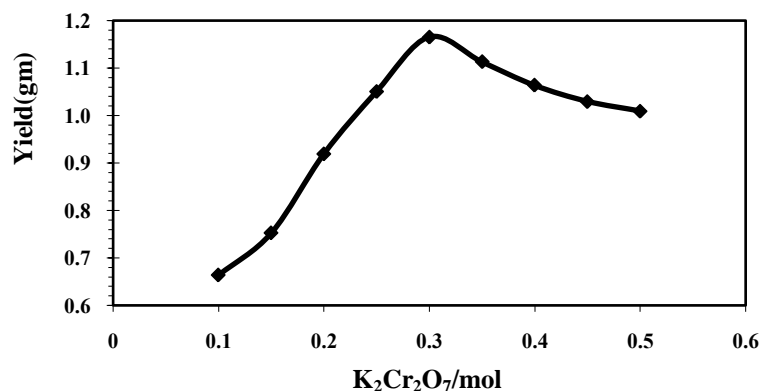
Figure (1)-Yield -$K_2Cr_2O_7$ concentration effect on the aqueous oxidative polymerization of poly- o-tolidine (POTO).

3.1.2. Effect of HCl concentration.

Oxidative chemical polymerization of substituted-aniline can occur within a very wide interval range of acidity. However, the oxidation products formed at different pH intervals possess radically different properties (I.Y. Shishov, (2012)). Polymerization in basic, neutral and weakly acidic media gives brown powder while in highly acidic medium conducting dark-green emeraldine can be obtained (Sayyah & Abd El Salam, (2006)).

The effect of HCl concentration on the aqueous oxidative polymerization of OTO was investigated using constant concentration of $K_2Cr_2O_7$ at 0.3M, monomer concentration at 0.1M and using different concentrations of HCl at 5±0.2°C. The yield –time curve was represented in figure (2). From which it is clear that, obtained yield increases in the acid concentrations range from 0.05 to 0.2 then decreases gradually up to 0.5M. This behavior may be due to, at higher concentration of HCl, the degradation of the polymer in the early stages of the reaction, which may be due to the hydrolysis of polyemeraldine chain (P.Chowdhury, (2005)) (S. M. Sayyah A. B., (2014)).
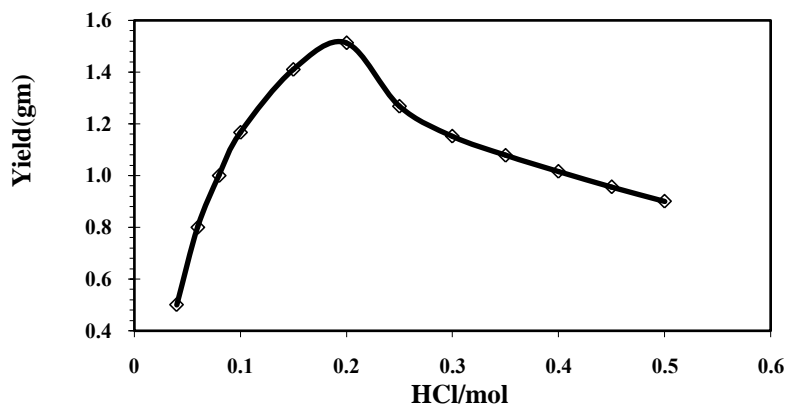
Figure (2)-Yield -HCl concentration effect on the aqueous oxidative polymerization of poly- o-tolidine (POTO).

3.1.3. Effect of o-tolidine concentration:

The effect of monomer concentration on the polymerization yield was investigated in the range of monomer concentrations from 0.05 to 0.5M and the data was represented in figure (3). From which it is clear that, the optimum yield formation is obtained at 0.1M of the monomer concentration.
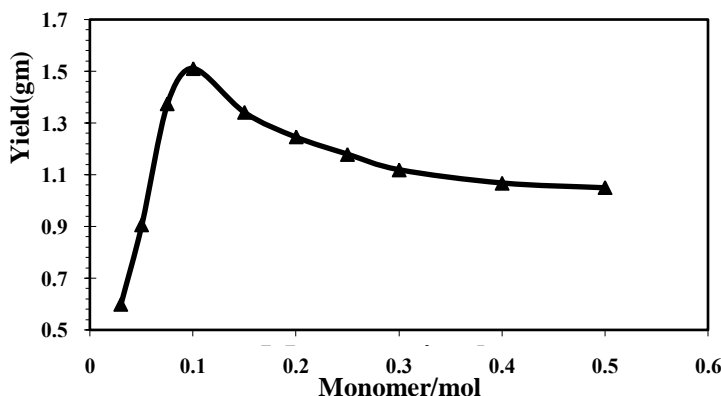
Figure (3)-Yield -monomer concentration effect on the aqueous oxidative polymerization of poly- o-tolidine (POTO).

3.2-The kinetic study of the polymerization reaction:

Study of o-tolidine polymerization in acidic aqueous media has shown that, the oxidation of monomer proceeds non-monotonically. It starts with a slow process ("induction period"); during this period, o-tolidine oligomers are formed. The induction period is followed by the rapid exothermic step of polymer chain propagation. This step is followed by termination of the reaction by addition of ammonium hydroxide solution in an equimolar amount to HCl present in the reaction medium

3.2.1- Effect of potassium dichromate concentration:

The aqueous polymerization of OTO (0.1 mol) was carried out in 25 ml of HCl solution (0.1 mol) in the presence of 25 ml potassium dichromate as oxidant of different molarities at 5 ^{0}C for different time intervals. The yield-time curves were plotted for different oxidant concentrations and the data are graphically represented in figure (4-a). The initial and overall reaction rates were determined using equation (5). Figure (4-a) shows that, the initial and overall reaction rate of the polymerization reaction increases with the increase of oxidant concentration in the range between 0.05 - 0.3 mol/l. The oxidant exponent was determined from the relation between logarithm of the initial rate of polymerization Log (R_i) against logarithm of the oxidant concentration. A straight line was obtained which has a slope of 0.927 as represented in figure (4-b). This means that the polymerization reaction of OTO is a first order reaction with respect to the oxidant.

3.2.2- Effect of hydrochloric acid concentration:

The polymerization of OTO (0.1 mol) in 25 ml of HCl with different molarities was carried out by addition of 25 ml potassium dichromate (0.3mol/L) as oxidant at 5 ^{0}C for different time intervals. The concentration of the monomer and oxidant were kept constant during the study of the effect of HCl concentration on the polymerization reaction.

The experiments were carried out as described in section 2.2, and the yield-time curve was plotted for each acid concentration used. The data are graphically represented in figure (5-a), from which it is clear that both the initial and overall reaction rates of the polymerization reaction increase with the increasing of HCl concentrations in the range between 0.05 - 0.2 mol/L. The HCl exponent was determined from the slope of the straight line represented in figure (5-b) and it is found to be 0.984, which means that the polymerization order with respect to the HCl concentration is a first order reaction.

3.2.3 - Effect of monomer (OTO) concentration:

The aqueous polymerization of OTO was carried out in 25 ml of HCl solution (0.2mol/L) in the presence of 25 ml potassium dichromate (0.3mol/L) as oxidant at 5 ^{0}C for different time intervals. The yield-time curve is plotted for each monomer concentration used. The data are graphically represented in figure (6-a). The monomer exponent was determined from the slope of the straight line represented in figure (6-b) for the relation between log R_i and logarithm of the monomer concentration. The slope of this linear relationship is found to be 1.086. This means that the polymerization reaction with respect to the monomer concentration is a first order reaction.

3.3-Calculation of the thermodynamic activation parameters:

The polymerization of OTO (0.1 mol/L) in 25 ml of 0.2 mol/L HCl in presence of 25 ml potassium dichromate (0.3 mol/L) as oxidant solution was carried out at 5, 10 and 15 ^{0}C for different time intervals. The yield-time curve was graphically represented in figure (7), from which it is clear that both of the initial and overall reaction rates increase with raising the reaction temperature. The apparent activation energy (E_a) of the aqueous polymerization reaction of o-tolidine was calculated using equation (6). By plotting log R_i against 1/T, which gave a straight line as shown in figure (8) and from the slope we can calculate the activation energy.
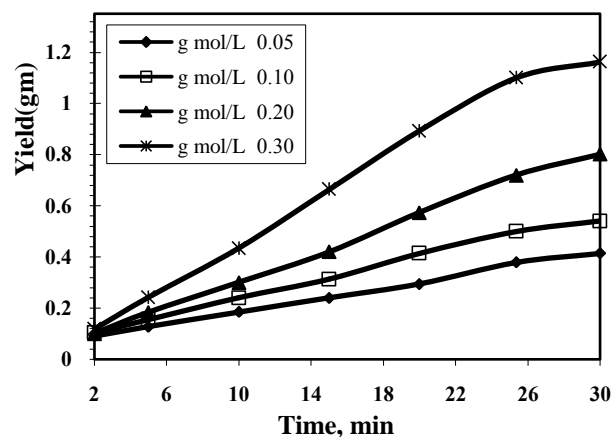
Figure (4-a)-Yield -time curve for the effect of potassium dichromate concentration on the polymerization of (POTO) at different time intervals.

Figure (4-b)-Double logarithmic plot of the initial rate and oxidant concentration of (POTO).

Figure (5-a)-Yield -time curve for the effect of HCl concentration on the polymerization of (POTO) at different time intervals.
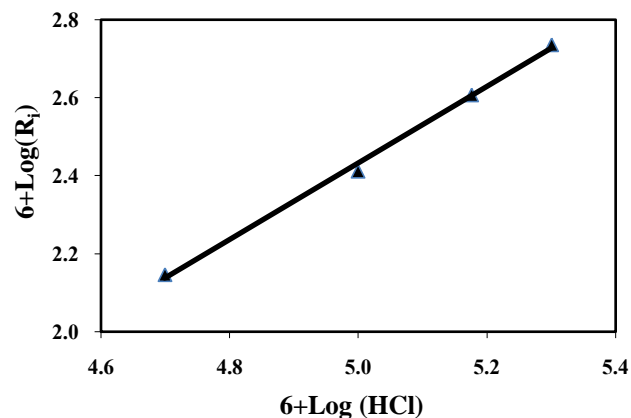
Figure (5-b)-Double logarithmic plot of the initial rate and HCl concentration of (POTO) .

591
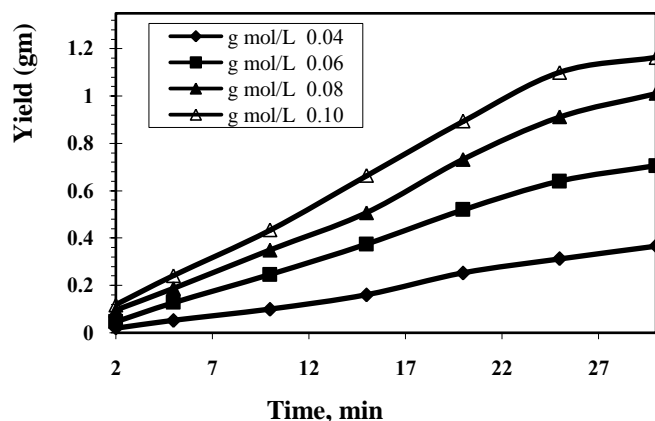
Figure (6-a)-Conversion -monomer/mol concentration effect on the aqueous oxidative polymerization of (POTO) at different time intervals.
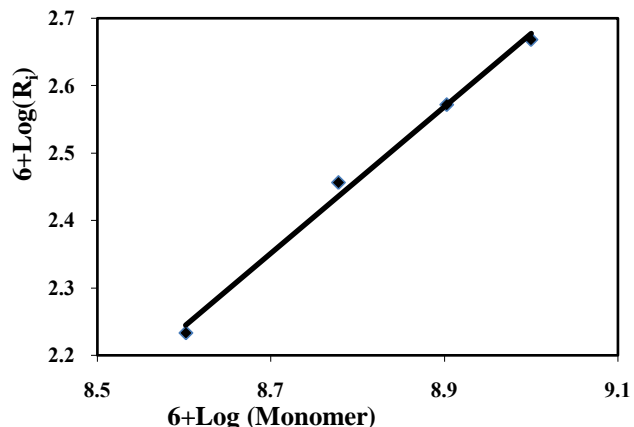
Figure (6-b)-Double logarithmic plot of the initial rate and monomer concentration of (POTO).

The apparent activation energy for this system is 59.26 kJ/mol. The enthalpy and entropy of activation for the polymerization reaction can be calculated by the calculation of K_2 from the following equation:

$$\text{Reaction Rate} = K_2 \text{[oxidant]}^{0.927} \text{[HCl]}^{0.984} \text{[monomer]}^{1.086} \tag{9}$$

The values of K_2 at 5, 10 and 15 ^{0}C were 5.37×10^{-6}, 10.25×10^{-6} and 13.13×10^{-6} respectively. The enthalpy (ΔH^*) and entropy (ΔS^*) of activation associated with K_2, were calculated using Eyring equation:

$$K_2 = (RT/Nh) \, e^{\Delta S^*/R} \cdot e^{-\Delta H^*/RT} \tag{10}$$

Where K_2 is the rate constant, N is the Avogadro's number, R is the universal gas constant and h is planks constant.

By dividing the above equation by T and taking its natural logarithm we obtain the following equation:

$$\text{Ln}(K_2/T) = \ln(R/Nh) + (\Delta S^*)/R + (-\Delta H^*)/RT \tag{11}$$

Figure (9) shows the relation between K_2/T vs $1/T$, which gives a linear relationship with slope equal to $(-\Delta H^*)/R$ and intercept equal to (ln R/Nh $+\Delta S^*/R$). From the slops and intercept, the values of ΔH^* and ΔS^* were calculated and it is found to be 84.05 kJmol^{-1} and 24.80 Jmol^{-1}K^{-1} respectively.

The activated complex formation step which is endothermic as indicated by the rate constant of polymerization seems to compensate each other. This fact suggests that the factors controlling ΔH^* must be closely related to those controlling ΔS^*. Therefore, the salvation state of the encounter compound could be important in determination of ΔH^*. Consequently, the relatively small enthalpy of activation can be explained in terms of the formation of more solvated complex.
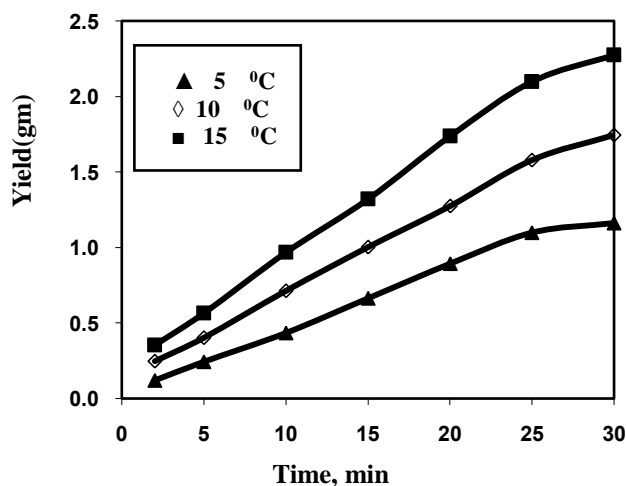
Figure (7)-Yield -time curve for the effect of temperature on the aqueous oxidative of (POTO).
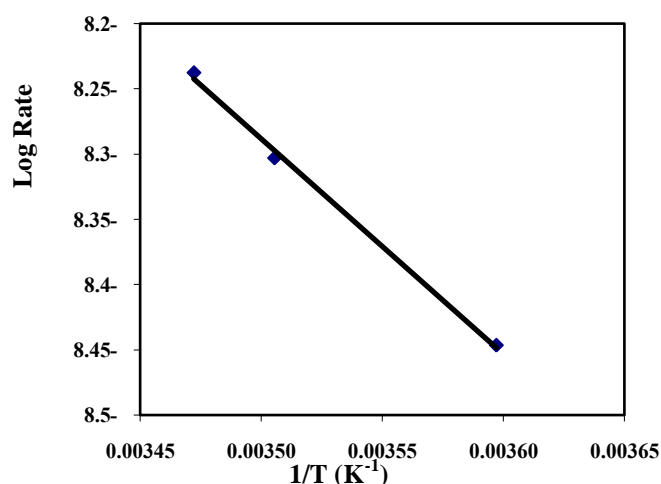
Figure (8): The relation between the logarithm of initial rate and (1/T) for aqueous oxidative polymerization of (POTO).
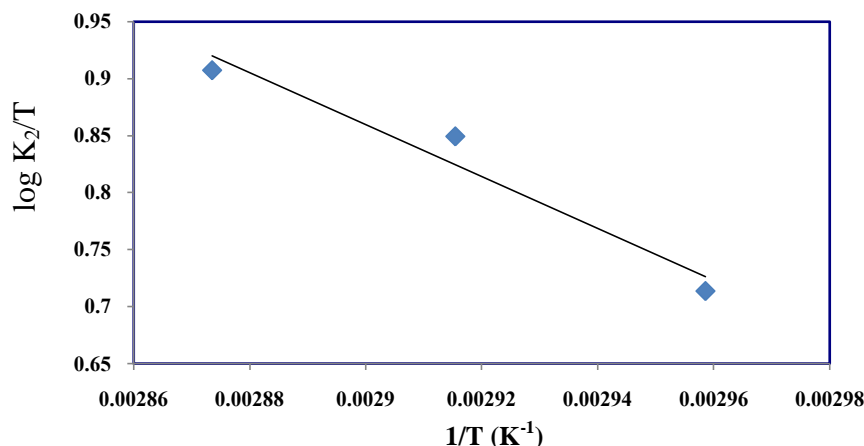
Figure (9): The relation between log K_2/T with 1/T for (POTO).

3.4-Polymerization mechanism:

The aqueous oxidative polymerization of o-tolidine is described in the experimental section, and follows three steps (Sayyah & Abd El Salam, (2006)).

The Initial Step

Potassium dichromate in acidified aqueous solution produces chromic acid as shown in equation (12):

$$K_2Cr_2O_7 + H_2O + 2H^+ = 2K^+ + 2H_2CO_4 \tag{12}$$
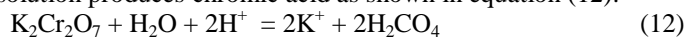
This reaction is controlled by the change in pH, the orange red dichromate ions $(Cr_2O_7)^{2-}$ are in equilibrium with the $(HCrO_4)^-$ in the range of pH-values between 2 and 6, but at pH below 1 the main species is (H_2CrO_4) and the equilibria can occur as follows:

$$(HCrO_4)^- \rightleftharpoons (CrO_4)^{2-} + H^+ \qquad K = 10^{-5.9} \tag{13}$$

$$(H_2CrO_4) \rightleftharpoons (HCrO_4)^- + H^+ \qquad K = 4.1 \tag{14}$$

$$2(HCrO_4)^- \rightleftharpoons (Cr_2O_7)^{2-} + H_2O \qquad K = 10^{-2.2} \tag{15}$$
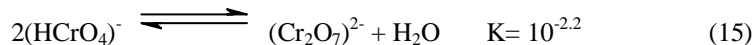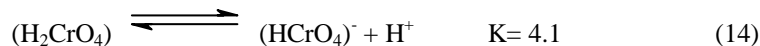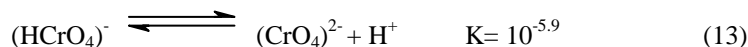
The chromic acid withdraws one electron from each protonated OTO and probably forms a metastable complex as shown in equation (16):
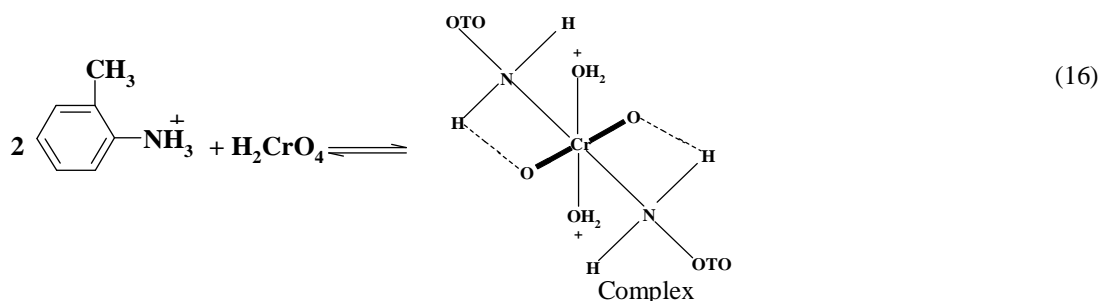
The complex undergoes dissociation to form monomer cation radical as shown in equation (17):
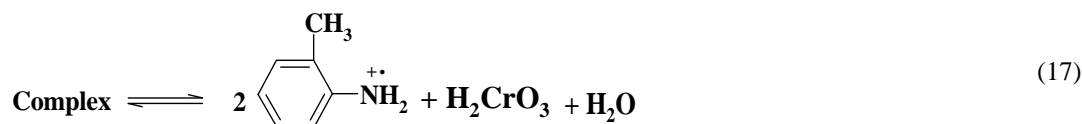
Generally, the initial step is rapid and may occur in short time, 0–5 min (autocatalitic reaction).

Propagation Step

This step involves the interaction between the formed radical cation and the monomer to form a dimer radical cation. In the case of Cr (VI) oxidation of the organic compounds, Cr (VI) is reduced to Cr (IV) first and then to Cr (III) (Sayyah & Abd El Salam, (2006)). Transfer of two electrons from two monomer ion radical by H_2CrO_4 produces para semidine salt along with chromous acid $H_2Cr_2O_3$ (Cr (IV)). The intermediately produced Cr (IV)

oxidizes para semidine to pemigraniline salt (PS) at suitable low pH and the PS acts as a catalyst for conversion of OTO to POTO.

$$2 \text{ (o-toluidine radical cation) } + H_2CrO_4 = \text{ (parasemidine) } + H_2CrO_3 + H_2O \qquad (18)$$

parasemidine

$$\text{ (pemigraniline radical) } + 2\,H_2CrO_3 + 6\,H^+ = \text{ (product) } + 2\,Cr^{+3} + 6\,H_2O \qquad (19)$$

Pemigraniline salt
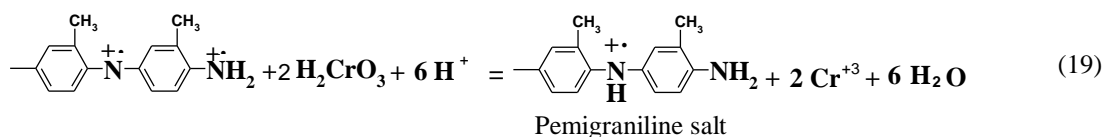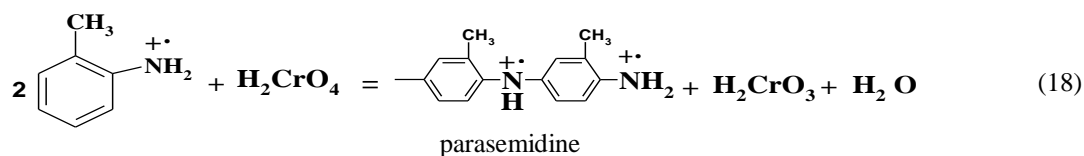
This reaction is followed by further reaction of the formed dimmer radical cations with monomer molecules t o form trimer radical cations and so on. The degree of polymerization depends on different factors such as dichromate concentration, HCl concentration, monomer concentration, and temperature. By adding equations 12, 16, 17, 18 and 19.

$$2 \text{ (o-toluidine) } + K_2Cr_2O_7 + 8\,H^+ = PS + 2K^+ + 2Cr^{3+} + 7\,H_2O \qquad (20)$$

$$12\ OTO + 5\ K_2Cr_2O_7 + 34\ H^+ = 6\ PS + 10\ Cr^{3+} + 10\ K^+ + 35\ H_2O \qquad (21)$$
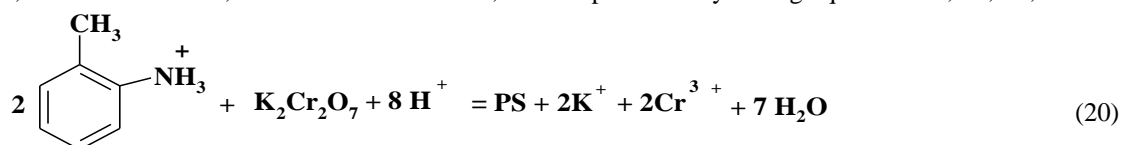
Termination Step

Termination of the reaction occurs by the addition of ammonium hydroxide solution in an equimolar amount to HCl present in the reaction medium (till pH = 7), which leads to cessation of the redox reaction. The reaction could occur as follows:
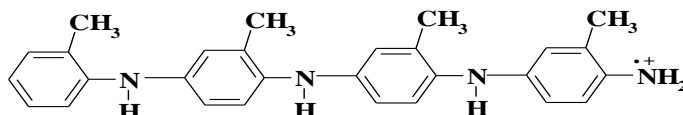
3.5 Characterization of the obtained polymer:

3.5.1 The solubility:

Poly aniline has low solubility in most polar and non-polar solvents (S. M. Sayyah S. S.-R.-D., (2010),). The solubility of (POTO) was investigated in N-methyl pyrrolidone, dimethylformamide (DMF), acetone, methanol, iso propanol, benzene, hexane and chloroform. The solubility values are listed in table (1). The (POTO) completely soluble in N-methyl pyrrolidone and slightly soluble in DMF, acetone, methanol and iso propanol at 20 ^{0}C but not soluble in benzene, hexane and chloroform.

Table (1): Solubility of poly- o-tolidine (POTO) in different solvents at 20 ^{0}C.

Solvent	Solubility of (POTO) in (g/l)
N-methyl -2-pyrrolidone	**Completely soluble**
Dimethylformamide	**2.425**
Acetone	**1.756**
Methanol	**1.102**
Iso propanol	**0.892**

3.5.2The elemental analysis:

The data obtained from elemental analysis using oxygen flask combustion and a dosimat E415 titirator shows that, the found carbon content of (POTO) is lower than the calculated value. This is due to the formation of chromium carbide during step of heating and measuring process while the found value of nitrogen and hydrogen are 10.95 and 5.54 respectively which are in good agreement with the calculated one for the suggested structure present in scheme (1). By measuring another sample of the (POTO) which was prepared by using ammonium persulfate as

oxidant the found value of carbon, is higher than sample which, is prepared by using potassium dichromate as oxidant (S. M. Sayyah A. B., (2014)). For more information about the chemical composition of (POTO), the XPS study was conducted as mention under point 3.5.2
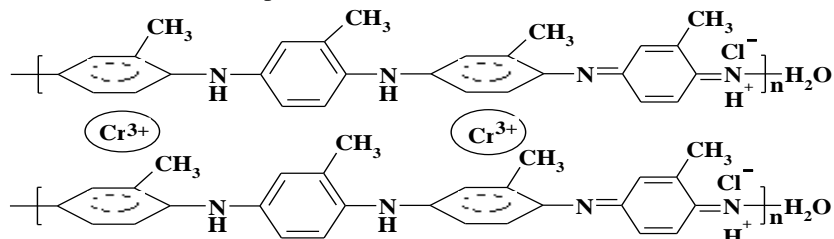
Scheme (1).Structure of the prepared poly o-tolidine (POTO).

3.5.3. -X-Ray Photoelectron Spectroscopy (XPS) characterization:
3.5.3. 1- XPS survey elemental composition:

X-Ray Photoelectron Spectroscopy (XPS) is used to study the composition of materials, which detect elements starting from Li (Z=3) and higher elements. Hydrogen (Z = 1) and helium (Z = 2) cannot be detected due to the low probability of electron emission. XPS survey begins from 0 to 1300 (eV) as shown in figure (10). The XPS survey scan spectrum of the prepared polymer shows the presence of C, N, O, Cl and Cr. The Cl is present as doping anion in the prepared polymer. It is possible for chromium ion (Cr^{+3})to present between polymer chains as a sandwich-bonded C_6H_6-C_6H_6 groups as shown in scheme (1) and the usual formation procedure is the hydrolyze the reaction mixture with dilute acid which gives the cation $(C_6H_6)_2Cr^{3+}$ (F.Cotton) (H.Zeiss., (1966)).

The XPS elemental analysis of the prepared polymer is given in table (2). The data shows that there is a good agreement with the calculated one for the suggested structures present in scheme (1).

Table (2): The XPS elemental analysis of poly-o-tolidine (POTO).

C %		N %		Cl %		O %		Cr %	
Calc.	Found	Calc.	Found	Calc.	Found	Calc.	Found	Calc.	Found
67.82	68.11	11.30	11.74	7.17	6.81	3.23	3.11	10.48	10.23
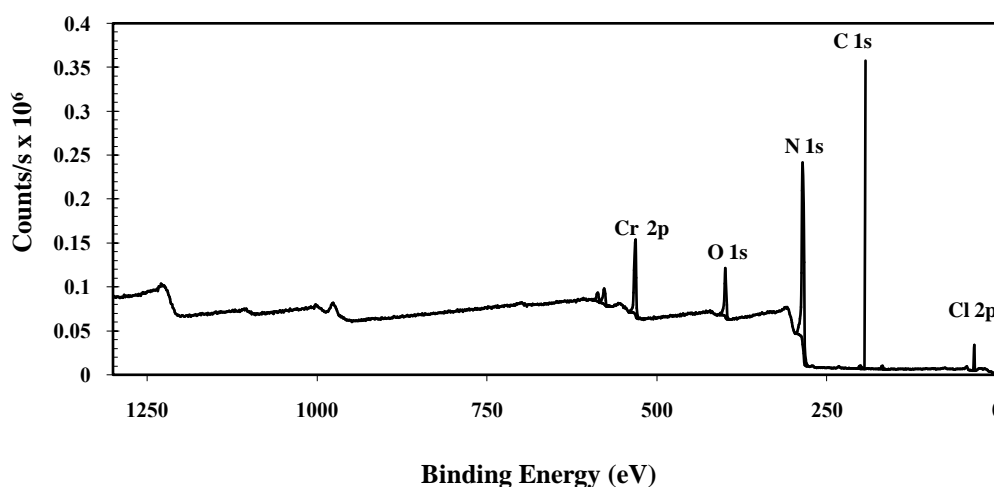
Binding Energy (eV)
Figure (10):X-Ray Photoelectron Spectroscopy (XPS) survey elemental composition of (POTO).

3.5.3.2- XPS spectra of poly (OTO):

Three main peaks were obtained for C1s spectra of poly (OTO) as shown in Figure (11-a). The sharp peak appearing at 284.29 eV is attributed to C-C bond. The peak appearing at 287.53 eV is assigned to C=N bond while, the peak appearing at 288.48 eV is attributed to C-O or C-N^+ (C_3) bond (A.Qaiser., (2012)) (J.Li., (2010)) (K.Tan, (1991)).

N1s Figure (11-b) shows the XPS N1s spectrum of poly (OTO) which has distinct peak at about 398.86 eV , characteristic of the –NH- structure of sponges and insure presence of steric strain associated with the amine group. The steric strain may be relieved by sequestration of proton from –CH_3 which lead to the formation of very stable ionic complex containing hydrogen bond N-H-N^+ bride (S.J.Kerber., (1996)).

Two distinct oxygen species contributes to the oxygen 1s signals in the conducting polymers (Figure (11-c)). The distinct energy peaks at 530.68 and 533.12 eV could be attributed to Cr_2O_3 and C-OH respectively.

The Cl 2p spectrum of poly (OTO) is shown in figure (11-d). In order to estimate the anion Cl at the surface, Cl 2p peaks are fitted with a number of spin-orbit doublets (Cl $2p_{1/2}$ and Cl $2p_{3/2}$) doublets with the B.E. for the C12$p_{3/2}$ peaks at about 199.88 eV. This peak is attributed to the ionic and covalent chlorine species (Cl$^-$ and -Cl).

The Cr spectrum of (POTO) is shown in Figure (11-e). The main components corresponding to different chemical chromium species were observed in the high-resolution $Cr_2p_{3/2}$ spectrums. The first peak at 577.06 eV ± 0.2 eV was assigned to Cr_2O_3 which is in agreement with what was found by (P.Chowdhury, (2005)) and (P.Stefanov., (2000)) , also indicated by a distinct O1s peak at 530.68 eV typical for Cr_2O_3 which may be adsorbed on polymer surface during chromous acid $H_2Cr_2O_3$ oxidation process. There is also a component visible correspond to $Cr_2p_{1/2}$ at 586.34 eV, which was attributed to Cr^{3+}. This data reveal that, chromium ion present between benzene rings of polymeric chain as shown in scheme (1).
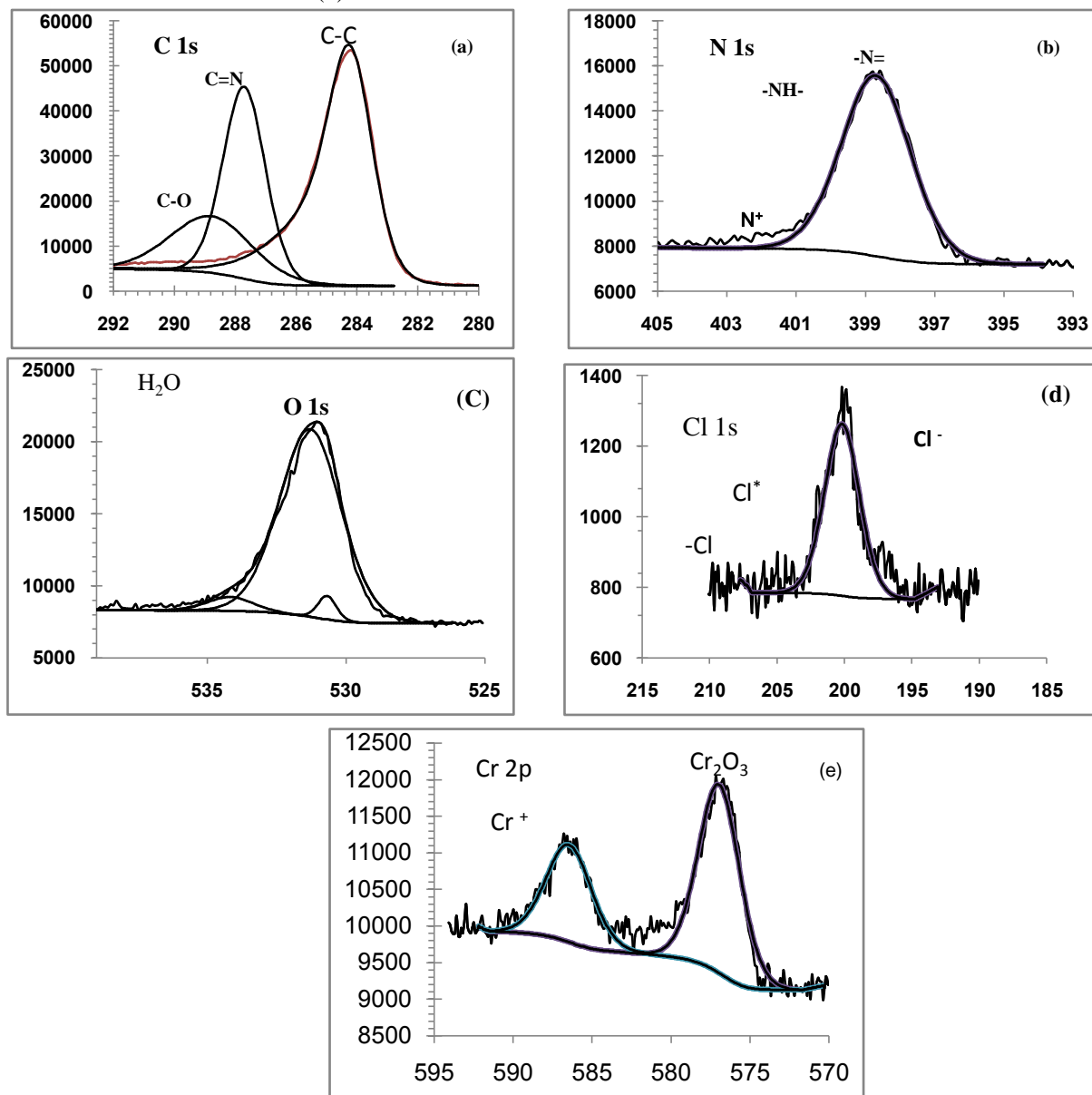
Binding energy (eV)
Figure (11):X-Ray photoelectron spectroscopy (XPS) spectra of (POTO).

3.5.4. The infrared spectroscopic analysis of (OTO) monomer and its analogs polymer:

The IR spectra of the OTO and its polymer (POTO) are represented in Figure (12), while the absorption band values and their assignments are summarized in table (3). The medium absorption band appearing at 538 cm^{-1} which could be attributed to bending deformation of N-H group attached to benzene ring in case of monomer, appears at 538 cm^{-1} in case of polymer. A series of absorption bands appearing in the region from 708 …. 983 cm^{-1} which could be attributed to the out of plane C-H deformation of 1,2-disubistuition benzene ring, in case of monomer and 1,2,4 tri-substituted benzene ring, in case of polymer. The medium absorption bands appearing at 1036 and 1100 cm^{-1} in case of monomer which could be attributed to the out of plane C-H deformation of 1,4-disubstituted benzene ring, appears as abroad band at 1033 and 1050cm^{-1} in case of polymer. A series of absorption bands appearing in the region from 1268 …. 1386 cm^{-1} which could be attributed to symmetric stretching vibration for C-O and C-N groups in both cases (monomer and polymer). The two sharp absorption bands appearing at 1500 and 1615 cm^{-1} in case of the monomer , appears also as two splitted bands at 1560 and 1633 cm^{-1} in case of polymer , which could be attributed to stretching vibration for C=C in aromatic rings. The two shoulder bands appearing at 2840 and 2933 cm^{-1} in case of the monomer, appears as a broad band at 2923 cm^{-1} in case of the polymer, may be attributed to symmetric stretching vibration of N-H. The sharp absorption band appearing at 3369 cm^{-1} which could be attributed to asymmetric stretching vibration for NH group in case of monomer, appears as abroad absorption band at 3424 cm^{-1} in case of polymer.
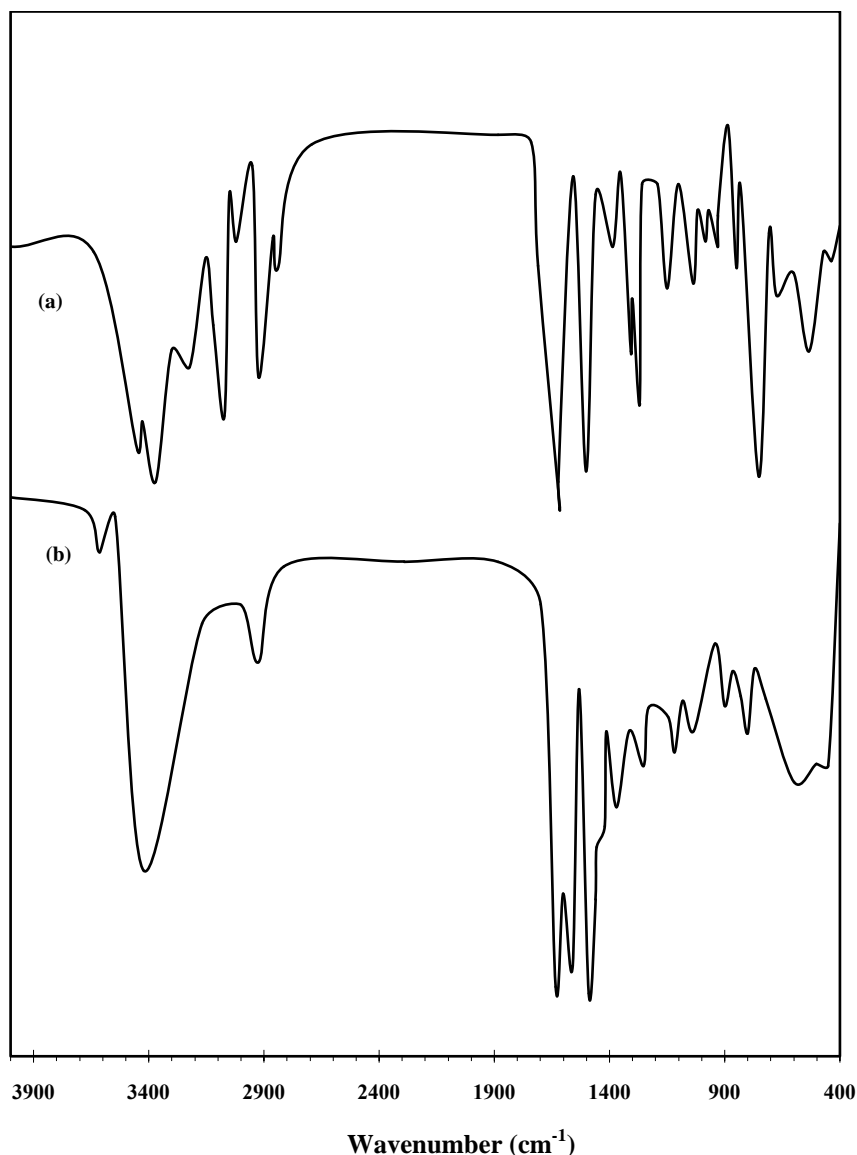
Figure(12):The infrared spectrum of (OTO) (a) and it analogous polymer (POTO) (b).

597

Table (3): Infrared absorption bands and their assignments of o-tolidine monomer and its analogs polymer.

Wave number(cm^1)		Assignments
Monomer	Polymer	
43 6^m	—	Bending deformation of N-H group attached to benzene ring
538 ^{m}	538^b	
708^{sh}	—	Out of plane C-H deformation of 1,2-disubistuition of benzene ring, in case of monomer and 1,2,4 tri-substituted of benzene ring, in case of polymer.
752^s	—	
—	754^b	
850^w	—	
—	860^w	
930^w	—	
983^w	750^b	
1036^b	1033b 1050^b	Out of plane C-H deformation of 1,4-disubistuition of benzene ring
1063^{sh}		
1150^s	1150^{sh}	
—	1247^b	Symmetric stretching vibration for C-O and C-N groups
1269^s	—	
1307^{sh}	—	
1386^w	—	
1500^s	—	Stretching vibration for C=C in aromatic system
—	1560^s	
1615^s	1633^{sh}	
2840^{sh}	—	Symmetric stretching vibration of N-H
2933^s	2924^b	
3024^s	—	Stretching vibration of C-H aromatic
3222^{sh}	—	
3369^s	—	Asymmetric stretching vibration for NH group
—	3424^b	
3450^b		
3612^w	—	Stretching vibration of free OH group

s= sharp   m= medium   w=weak   b=broad   sh=shoulder

3.5.5. The UV-visible Spectroscopic Study of (OTO) monomer and its analogs polymer:
The UV-visible spectra of OTO and its polymer are represented in figure (13); the spectra show the following absorption bands:

(1) In case of monomer, two absorption bands appear at λ_{max} = 206 and 216.4 nm which may be attributed to π-π^* transition (E_2-band) of the benzene ring and the β-band ($A_{1g} - B_{2u}$).

(2) In case of polymer, two absorption bands appear at λ_{max} = 207.5 and 281 nm which may be attributed to π-π^* transition showing a bathochromic shift. Beside these two bands, broad absorption band appears in the visible region at λ_{max} = 526 nm which may be due to the high conjugation of the aromatic polymeric chain.
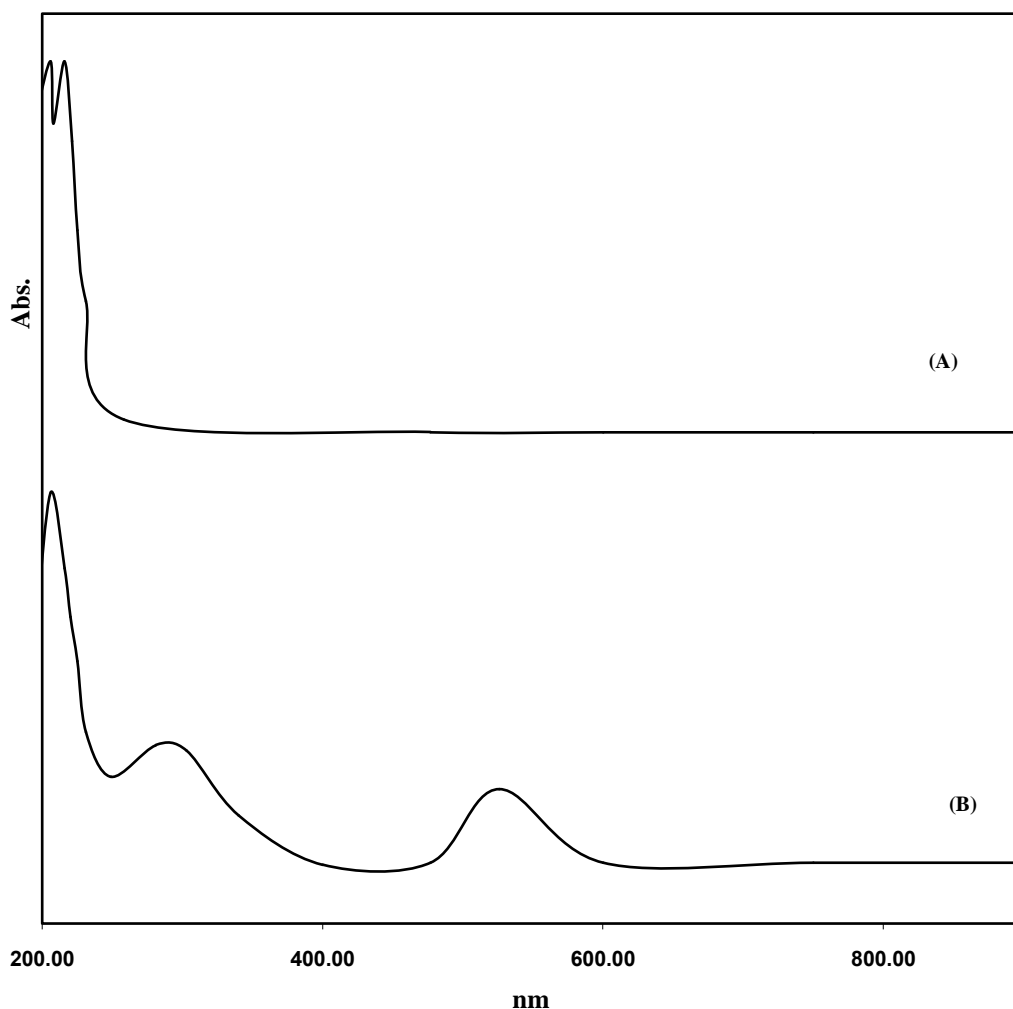
Figure (13):UV-visible spectra of (OTO) (A) and it analogous polymer (POTO) (B).

3.5.6-Thermal Gravimetric analysis (TGA) of poly o-tolidine:
Thermogravimetric analysis (TGA) for the prepared polymer has been investigated and the TGA-curve is represented in Figure (14). The calculated and found data for the prepared polymers are summarized in table (4). The thermal degradation steps are summarized as follows:

(1)The first stage includes the loss of one water molecule in the temperature range between 48.58-173.5 °C, the weight loss of this step was found to be 3.45 % which is in a good agreement with the calculated one (3.43 %).

(2)The second stage, in the temperature range between 173.5-470.6 °C the weight loss was found to be 6.95 %, which could be attributed to the loss of one HCl molecule. The found weight loss is in good agreement with the calculated one (6.96 %).

(3)The third stage, in the temperature range between 470.6-512.5 °C, the weight loss was found to be 11.92 %, which is attributed to the lost of 4CH$_3$. The calculated weight loss of this stage is equal to 11.44 %.

(4)The fourth stage, in the temperature range between 512.5-635.65 ^{o}C, the weight loss was found to be 33.82 %, which is attributed to the loss of two molecules of $2C_6H_3$-2NH. The calculated weight loss of this stage is equal to 34.13 %.

(5)The fifth stage, in the temperature range between 635.65-998.92 ^{o}C, the weight loss was found to be 34.05 %, which is attributed to the lost of two molecules of $2C_6H_3$-2N. The calculated weight loss of this stage is equal to 34.32%.

(6)The last stage, above 998.92 ^{o}C, the remained polymer molecule was found to be 10.89 % including the metallic residue but the calculated one was found to be 10.22 %.
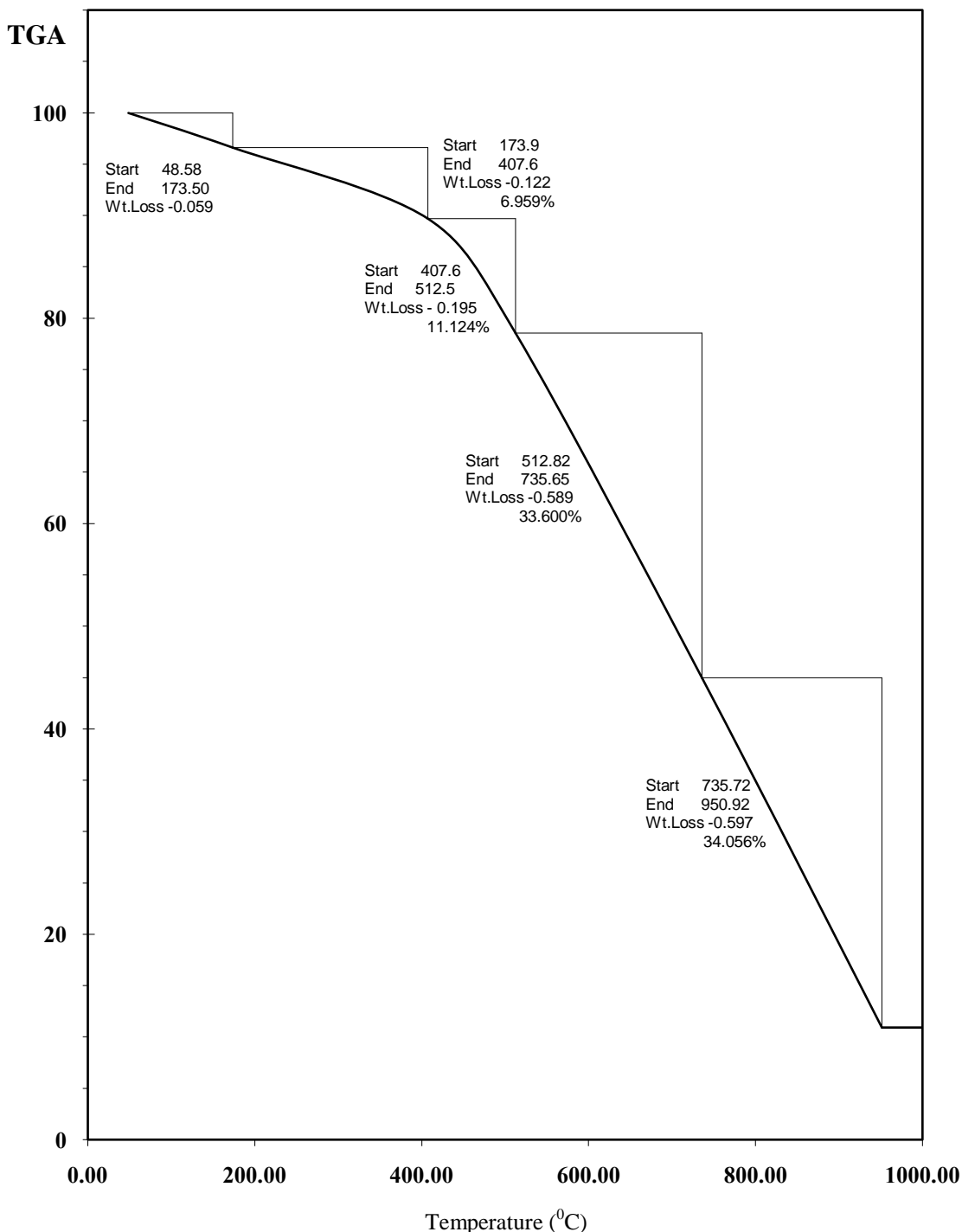
Figure (14): The thermal Gravimetric analysis (TGA) for(POTO).

600

Table (4): Thermogravimetric data of poly- o-tolidine (POTO).

Name	Temperature range ^0C	Weight loss (%)		The removed molecule
		Calc.	Found	
Poly (POTO)	48.5-173.5	3.43	3.45	H_2O
	173.5-470.6	6.96	6.96	HCl
	470.6-512.5	11.44	11.92	$4CH_3$
	512.5-635.65	34.13	33.82	$2C_6H_3$-2NH
	635.65-998.92	34.32	34.06	$2C_6H_3$-2N
	Remaining weight(%) above 998.92	9.706	9.791	……..

3.5.7 -The X-Ray diffraction analysis and transimation electron microscope:

The X-Ray diffraction Patterns of the prepared polymer is represented in figure (15). The figure shows that, the prepared poly o-tolidine is completely amorphous.

Morphology of MWCNTs, poly o-tolidine and POTO/ MWCNTs composite was characterized by transmission electron microscope. Figure (16-(a)) indicates tubular structure of MWCNTs and TEM images shows that, they had internal diameters of approximately 12–15 nm and external diameters of 55–68 nm. Their outer walls were very deformed since amounts of amorphous carbon were deposited on them. Figure (16-(b)) shows TEM image of poly o-tolidine which shows spherical or ellipsoidal particles with approximate diameter 249-310 nm either separated or linked with each other. Figure (16-(C)) shows TEM image of POTO/ MWCNTs composite. TEM image indicates that, some polymer particle polymerized on the surface of CNTs and others polymerized inside CNTs, leading to swelling of CNTs and the external diameters increase to approximately 50–103 nm.
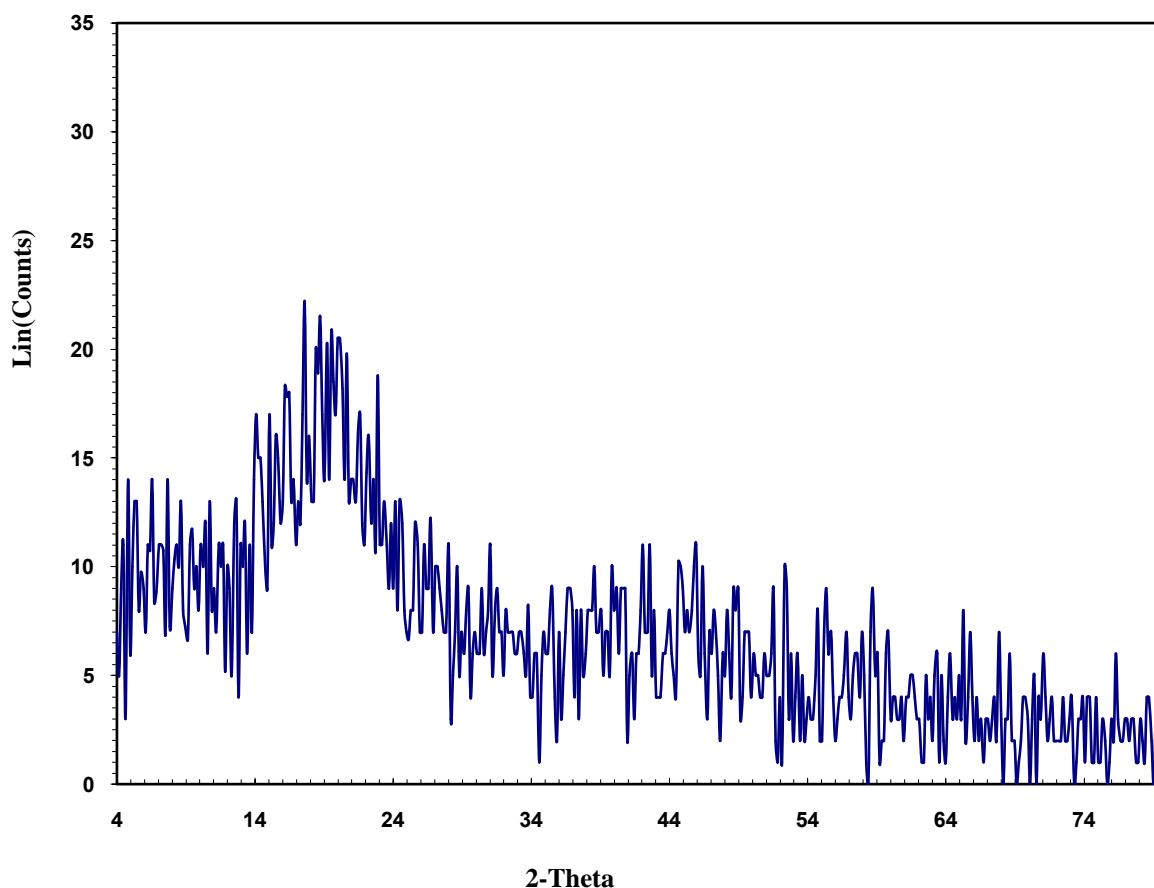
Figure (15):X-ray of poly- o-tolidine (POTO).

(a)   (b)   (c)
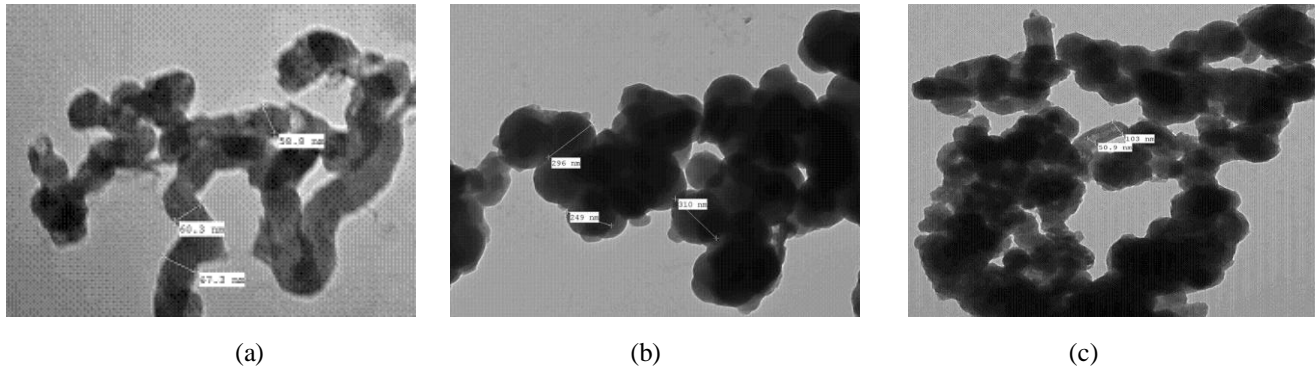
Figure (16): The transimation electron microscope of MWCNTs (a), (POTO) (b) and POTO/ MWCNTs(c) composite.

3.6. Dielectric properties and a.c conductivity (σ_{ac}) measurements:

Figure (17) shows the variation in dielectric constant ($\acute{\varepsilon}$) of POTO as a function of frequency at room temperature. It is clear that $\acute{\varepsilon}$ decrease sharply up to a certain frequency after which it becomes nearly constant. This behavior has also been observed by (Rahaman, (2012)) , (Sohi, (2011)) and (Pant) and could be attributed to the frequency dependent of the polarization processes. He same behavior is recorded for higher temperatures. This can be explained on the basis of the fact that after some frequency value, field reversal becomes so fast that dipoles are unable to orient themselves and intrawell hopping probability of charge carriers dominates in rapid field reversal in such a small interval of time (A. K.Tomara., (2012)).

Figure (18) reveals that dielectric loss ε'' decrease with increasing frequency. A decrease of ε'' orders of magnitude was observed when the frequency was increased from 0.1 kHz to 100 kHz. At low frequency, the high value of dielectric loss ε'' is usually associated with the motion of free charge carriers within the material, dipole polarization or interfacial polarization (A. K.Tomara., (2012)). At high frequency, periodic field reversal is so fast that there is no excess ion diffusion in the direction of electric field and thus, charge accumulates and polarization decreases due to accumulation of charges leading to the decrease in ε'' (C.Dyre., (1988)), (D.Mardare., (2004)).
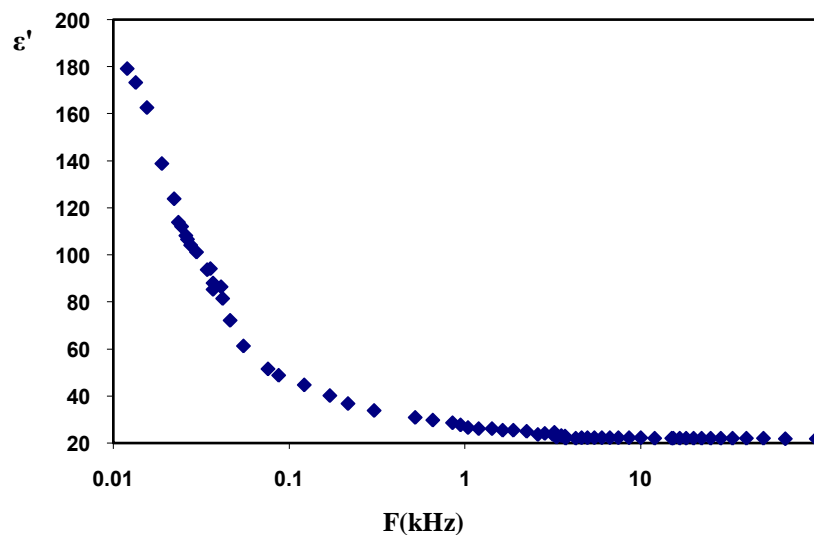
Figure (17): Variation of dielectric constant ($\acute{\varepsilon}$) of poly tolidine with frequency at room temperature.

Figure (19) represents the variation in ac conductivity (σ_{ac}) for (POTO) as a function of frequency and temperature. It is observed that, the value of ac conductivity increases with the increase of frequency. This behavior is in good agreement with the random free energy model proposed by (C.Dyre., (1988)). According to this model, conductance increases as a function of frequency in many solids, including polymers, which can be explained on the basis of any hopping model. The rise in conductivity upon increasing the frequency and temperature is common for disordered conducting polymer. As can be seen, each curve displays a conductivity dispersion, which is strongly dependent on frequency and shows weaker temperature dependent.
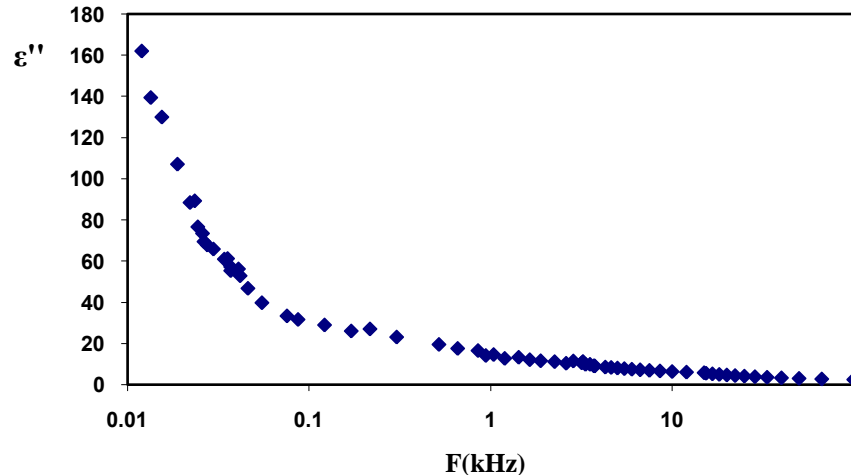
Figure (18): Variation of dielectric loss (ε″) of tolidine with frequency at room temperature.

The recorded conductivity value at room temperature of POTO was found to be 0.0352 S/cm which is higher than conductivity of polyaniline–polyvinyl alcohol blends 10.5×10^{-5} Scm^{-1} (P. Dutta., (2001)) and ac conductivity of HCl doped polyaniline synthesized by the interfacial polymerization technique 6.2×10^{-5} S cm^{-1} (P.Chutia, (2014)). Also, the ac conductivity of POTO is higher than polyaniline loaded with 10 % molybdenum trioxide composites 0.025 s/cm (K.R.Anilkumar., (2009)) but lower than the determined value of ac conductivity of polyaniline prepared by $K_2Cr_2O_7$ as oxidant 1.922 S cm^{-1}. Such difference could be attributed to the different disorder of each composite, substituted function group and using of different dopant.

In general, for amorphous conducting material, disordered systems, low mobility polymers and even crystalline materials, the ac conductivity (σ_{ac}) as a function of frequency can be obeys a power law with frequency (A.Paphanassiou., (2002)). The ac conductivity (σ_{ac}) over a wide range of frequencies can be expressed as:

$$\sigma_{ac}(\omega) = A\omega^s \qquad (17)$$

Where A is a complex constant and the index (s) is frequency exponent and ω is the angular frequency ($\omega = 2\pi f$).

Figure (19) shows the relation between Ln σ_{ac} and Ln ω at different temperatures.

The value of (s) at each temperature has been calculated from the slope of ln σ (ω) versus ln(ω) plot. As shown in figure (20) the calculated value of (s) for (POTO) sample is less than unity and decrease with temperature. The microscopic conduction mechanism of disordered systems are governed by two physical processes such as classical hopping or quantum mechanical tunneling of charge carries over the potential barrier separating two energetically favorable centers in a random distribution. The exact nature of charge transport is mainly obtained experimentally from the temperature variation of exponent (s) (Dey, De, & Sk, (2004)). The temperature exponent (s) dependences for (POTO) sample reveals that the frequency exponent (s) decreases with the increase of temperature. This behavior is only observed in the correlated barrier hopping model proposed by (Elliott, (1987)).
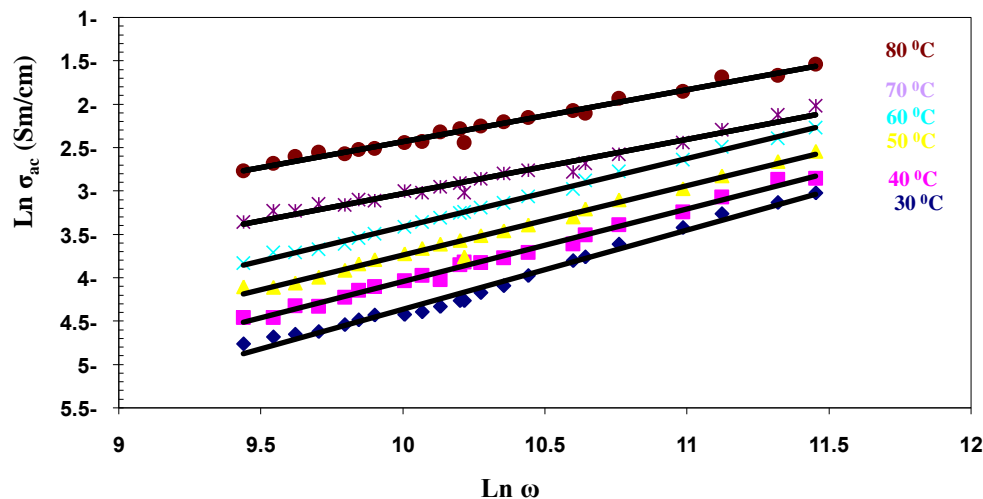
Figure (19): ac conductivity vs. angular frequency for (POTO) with frequency at different temperatures.
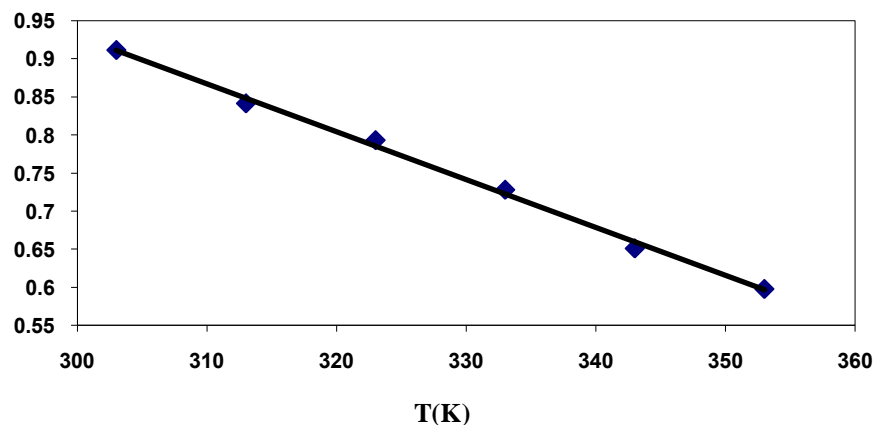
Figure (20): Frequency exponent (s) vs. temperature for (POTO).

Conclusion

In the present work POTO polymer prepared by chemical oxidative polymerization using potassium dichromate and HCl has been successfully achieved. The optimum yield formation of POTO is obtained by using 0.3M potassium dichromate, 0.1M of the monomer and 0.2M hydrochloric acid concentrations. The initial and overall rate of polymerization reaction increases with the increasing of the oxidant, monomer and HCl concentrations. The exponent of oxidant, monomer and HCl was found to be 0.927, 1.086 and 0.984 respectively. The chromium ions are present between polymer chains as a sandwich-bonded C_6H_6-C_6H_6 groups. The ac conductivity increase with the increase of frequency and temperature. The microscopic conduction mechanism of charge carries over the potential barrier in polymer backbone is a classical hopping model.

References

[1] Hrehorova, E., Bliznyuk,V.N., Pud, A.A., Shevchenko, V.V., Fatyeyeva, K.Y., (2007). Electrical properties and fractal behavior of polyurethane elastomer/polyaniline composites under mechanical deformation. Polymer, 48:4429-4437.

[2] Wang, P., Liua, L., Mengistiec, D. A., Li, K., Wen, B., Liue, T., and Chuf, C., (2013). Transparent electrodes based on conducting polymers for display applications. Displays, 34: 301–314.

[3] Jaymand, M., (2013). Recent progress in chemical modification of polyaniline. Prog. Polym. Sci.,38: 1287–1306.

[4] Guo, X., Baumgarten, M., and Müllen, K., (2013). Designing conjugated polymers for organic electronics. Prog. Polym. Sci., 38: 1832– 1908.

[5] Zhao, Y., Si, S., and Liao, C., (2013). A single flow zinc//polyaniline suspension rechargeable battery. Journal of Power Sources, 241: 449-453.

[6] Steffens, C., Manzoli, A., Oliveira, J. E., Leite, F. L., Correa, D. S., and Herrmann, P., (2014). Bio-inspired sensor for insect pheromone analysis based on polyaniline functionalized AFM cantilever sensor. Sensors and Actuators., B191: 643– 649.

[7] Wang, L., Hua, E., Liang , M., Ma, C., Liu, Z., Sheng, S., Min Liu , Xie, G., and Feng, W. (2014). Graphene sheets, polyaniline and AuNPs based DNA sensor for electrochemical determination of BCR/ABL fusion gene with functional hairpin probe. Biosensor, 51C:201-207

[8] Moon, Y., Yun, J., and Kim, H., (2013). Synergetic improvement in electromagnetic interference shielding characteristics of polyaniline-coated graphite oxide/g-Fe2O3/BaTiO3 nanocomposites. J. Ind. Eng. Chem., 19:493– 497.

[9] Gupta, G., Birbilis, N., Cook, A.B., and Khanna, A.S., (2013). Polyaniline-lignosulfonate/epoxy coating for corrosion protection of AA2024-T3. Corros. Sci., 67: 256–267.

[10] Elkais, A. R., Gvozdenovi´c, M. M., Jugovi´c, B.Z., and Grgur, B. N., (2013). The influence of thin benzoate-doped polyaniline coatings on corrosion protection of mild steel in different environments. Progress in Organic Coatings. 76: 670– 676.

[11] Guo, X., Baumgarten, M., Müllen, K., (2013). Designing π-conjugated polymers for organic electronics. Prog. Polym. Sci., 38: 1832– 1908.

[12] Gospodinova, N., and Terlemezyan, L., (1998). Conducting polymers prepared by oxidative polymerization :Polyaniline. Prog. Polym. Sci., 13:1443–1484.

[13] Gurunathan, K.,   Vadivel, A., Marimuthu, R., Mulik, U.P., and Amalnerkar,D.P., (1999). Electrochemically synthesised conducting polymeric materials for applications towards technology in electronics, optoelectronics and energy storage devices. Mater.Chem. Phys., 61: 173-191.

[14] Chowdhury, P., Saha, B., (2005). Potassium dichromate initiated polymerization of aniline. Indian. J. Chem. Technol. 12: 671-675.

[15] Hirase R, Shikata T, Shirai M. (2004). Selective formation of polyaniline on wool by chemical polymerization, using potassium iodate. Synth Met. 146(1):73-77.

[16] Gopalakrishnan, K., Elango, M., Thamilsevan, M., (2012). Optical studies on nano-structured conducting Polyaniline prepared by chemical oxidation method. Arch. Phys. Res., 3(4): 315.

[17] Molapo, K., Ndangili, P., Ajayi, R., Mbambisa, G., Mailu, S., Njomo, N., Masikini, M., Baker, P., Iwuoha, E., **(2012).** Electronics of Conjugated Polymers (I): Polyaniline Int. J. Electrochem. Sci., 7: 11859.

[18] Cao,Y., Smith, P., Heeger, A., (1992). Counter-ion induced processibility of conducting polyaniline and of conducting polyblends of polyaniline in bulk polymers. Synth. Met,. 48: 91-97.

[19] Heeger, **A.**, **(1993).** Polyaniline with surfactant counterions: conducting polymer materials which are processable in the conducting form .Synth. Met. 55: 3471-3482.

[20] Kang, Y.,   Lee, M., Rhee, S., (1992). Electrochemical properties of polyaniline doped with poly(styrenesulfonic acid. Synth. Met., 52: 319 -328.

[21] Pron, A., Laska, J., Osterholm, J., Smith, P., (1998). Processable conducting polymers obtained via protonation of polyaniline with phosphoric acid esters. Polymer. 34: 4235-4240.

[22] Sayyah, S.M., Abd-El Salam, H., Azzam., E.,(2005). Surface Activity of Monomeric and Polymeric (3-alkyloxy aniline) Surfactants. Int. J. Polym. Mater. 54: 541-555.

[23] Sayyah, S.M., Bahgat, A., and Abd El Salam, H.,(2002). Kinetic study of the polymerization of substituted aniline in aqueous solutions and charactrization of the polymer obtained. Int. J. Polym.Mater. 51(3): 291-304.

[24] Sayyah, S.M., A. Abd El Khalek., A. Bahgat., H.Abd El Salam., (2001). kinetic study of the chemical polymerization of substituted aniline in aqueous solution and characterization of the polymer obtained,part1:3-chloroaniline. int. J. Polym. Mater., 50: 197-202.

[25] Sayyah, S.M., Abd El Salama., H. (2003). Aqueous oxidative polymerization of N-methyle aniline in acid medium and characterization of the obtained polymer Int. J. Polym. Mater. 52: 1087-1111.

[26] Sayyah, S.M., Abd El Khalek, A., Abd El Salam, H., (2001). Kinetic studies of the polymerization of substituted aniline in aqueous solutions and characterization of the polymer obtained. J. Polym. Mater. 49:25-49.

[27] Sayyah, S.M., Abd el Salam,H., Bahgat, A., (2002). Aqueous oxidative polymerization of 3-methoxyaniline and characterization of its polymerJ. Polym. Mater. 51: 915-923.

[28] Sayyah, S.M., Bahgat, A., Abd El Salam, H., (2002). Kinetic studies of the aqueous oxidative polymerization of 3-hydroxyaniline and characterization of the polymer obtained.Int. Polym. Mater. 51: 291-314.

[29] Sayyah, S.M., Abd El Khalek, A., Bahgat, A., Abd El Salama, H., (2001). kinetic study of the chemical polymerization of substituted aniline in aqueous solution and characterization of the polymer obtained,part1:3-chloroaniline. int. J. Polym. Mater., 50: 197-208.

[30] Bandaru. P., (2007). Electrical properties and applications of carbon nanotube Structures. J Nanosci Nanotechnol . 7: 11–29.

[31] Goh, P.S., Ismail, A.F., and Ng, B.C., (2014). Directional alignment of carbon nanotubes in polymer matrices: Contemporary approaches and future advances. Composites, Part A 56:103–126.

[32] Bahgata, M., Farghali, A.A., El Rouby, W.M.A., Khedr., M.H. (2011)" Synthesis and modification of multi-walled carbon nano-tubes (MWCNTs) for water treatment applications" Journal of Analytical and Applied Pyrolysis ., 92(2), 307–313.

[33] Sayyah, S. M., Khaliel, A. B., Abood, A.A., and Mohamed, S.M., (2014). Chemical polymerization kinetics of poly-o-phenylenediamine and characterization of the obtained polymer in aqueous hydrochloric acid solution using $K_2Cr_2O_7$ as oxidizing agent. s.l. : Inter. J. Polym. Sci.,, (2014). pp. xxx-xxx. Vols. xxx.,.

[34] Shishov, I.Y., and Sapurina, M.A., (2012). Oxidative Polymerization of Aniline:Molecular Synthesis of Polyaniline and the Formation of Supramolecular Structures. INTECH, New Polymers for Special Applications, 251-312.

[35] Sayyah, S.M. and Abd El Salam, H. (2006). Oxidative Chemical Polymerization of Some 3-alkyloxyaniline Surfactants and Characterization of the Obtained Polymers. Int. J.Polym. Mater. 55: 1075-1093.

[36] Sayyah, S. M., Abd El-Rehim, S. S., Kamal, S. M., El-Deeb, M. M., Azooz. R. E., (2010). Electropolymerization Kinetics of a Binary Mixture of o-Phenylenediamine and 2-Aminobenzothiazole and Characterization of the Obtained Polymer Films. s.l. : Journal of Applied Polymer Science, 119: 252-264.

[37] S. M. Sayyah, A. B. Khaliel, A. A.Aboud and S.M.Mohamed. (2014). Chemical polymerization kinetics of poly-o-phenylenediamine and characterization of the obtained polymer in aqueous hydrochloric acid solution using $K_2Cr_2O_7$ as oxidizing agent. Inter. J, Polym. Sci.,, xx:xx-xx. http://dx.doi.org/10.1155/2014/520910

[38] F.Cotton. Advanced in Organic Chemistry,. Third, p. 745.

[39] Zeiss, H., Whealty, P., Winkler, H.. Benzoic Material Complexes. Ronald Press, (1966).

[40] Qaiser, A., Hyland, M., and Patterson, D., (2012). Effects of various polymerization techniques on PANI deposition at the surface of cellulose ester micro-porous membranes: XPS and electrical conductivity studies. Synth. Met., 162: 958-967.

[41] Li, J., Qian, X., Wang, L., and Xi, A., (2010). XPS characterization and percolation behavior of polyaniline-coated conductive paper. Bio Resources., 5(2): 712-726.

[42] Tan, K., and Tan, B., (1991).   The chemical nature of the nitrogens in polypyrrole and polyaniline: A comparative study by x-ray photoelectron spectroscopy. J. Chem. Phys.,. 94(8): 5382-5391.

[43] Kerber, S.J., Bruckner, J.J., and Wozniak, K., (1996). The nature of hydrogen in X-Ray Photoelectron spectroscopy: General pattern from hydroxides to hydrogen bonding. Material interface, Inc., Sussex, Wisconsin, 1314-1320.

[44] Stefanov, P., Stoychev, D., Stoycheva, M., and Marinova, T., (2000). XPS and SEM studies of chromium oxide films chemically formed on stainless steel 316 L. Mater. Chem. Phys. 65(2): 212-215.

[45] Rahaman, M., Chaki,T.K., Khastgir ,D.,(2012). Consideration of interface polarization in the modeling of dielectric property for ethylene vinyl acetate (EVA)/polyaniline conductive composites prepared through in-situ polymerization of aniline in EVA matrix. s.l. : European Polymer Journal, 48: 1241–1248.

[46] Sohi, N., Rahaman, M., Khastgir, D.,(2011). Dielectric property and electromagnetic interference shielding effectiveness of ethylene vinyl acetate based conductive composites: effect of different type of carbon fillers. Polym Compos.,32:1148–54.

[47] Pant, H.C., Patra, M.K., Negi, S.C, Bhatia, A, Vadera, S.R, Kumar, N. (2006). Studies on conductivity and dielectric properties of polyaniline–zinc sulphide composites. Bull Mater Sci ., 29:379–384.

[48] A. K.Tomara., M.Suman., C.Rishi Pal, and K. Shyam.,(2012). Structural and dielectric spectroscopic studies of polyaniline–poly(methylmethacrylate) composite films. s.l. : Synthetic Metals, 162: 820– 826

[49] Dyre, J. C., (1988). The random free energy barrier model for ac conduction in disordered solids. J. Appl. Phys., 64(5) :2456.

[50] Mardare, D., Rusu, G.I., and Optoelectron, J., (2004). Comparison of the dielectric properties for doped and undoped TIO2 thin film. Adv. Mater., 6(1): 333-336.

[51] Dutta, P., Biswas, S., Ghosh, M., De, S.K., Chatterjee. S., (2001). The dc and ac conductivity of the polyaniline-polyvinyl alcohol blends. Synthetic Metals, 122:455–461.

[52] hutia, P., Kumar. A., (2014). Electrical, optical and dielectric properties of HCl doped polyaniline nanorods. PhysicaB, 436: 200–207.

[53] Anilkumar, K.R., Parveen, A., Badiger, G.R., Prasad. M., (2009). Effect of molybdenum trioxide (MoO$_3$) on the electrical conductivity of polyaniline. PhysicaB, 404(12): 1664–1667.

[54] Paphanassiou. A., (2002). The power law dependence of the a.c. conductivity on frequency in amorphous solids. J. Phys. D. Applied. Phys. 35: 17.

[55] Dey, A., De, S. and Sk, D. (2004). Characterization and dielectric properties of polyaniline–TiO$_2$ nanocomposites . Nanotechnology. 15: 1277.

[56] Elliott, S. (1987). .c. conduction in amorphous chalcogenide and pnictide semiconductors Adv. Phys. 36: 135.